



Wiley Analytical Science

Virtual Conference

The 5th edition of the Wiley Analytical Science Conference starts November 8, 2022!

Featured Sessions:

- **Integration of X-ray microscopy and finite elements into a digital twin**

Thurs Nov 10, 10:00 - 10:30 AM EST / 4:00 - 4:30 PM CET

- **Optimization of Cryo TEM lamella preparation workflows to be faster and more accessible**

Wed Nov 16, 10:00 - 11:00 AM EST / 4:00 - 5:00 PM CET

events.bizzabo.com/WASconferenceFall2022



Seeing beyond



WILEY

Making Highly Elastic and Tough Hydrogels from Doughs

Guodong Nian, Junsoo Kim, Xianyang Bao, and Zhigang Suo*

A hydrogel is often fabricated from preexisting polymer chains by covalently crosslinking them into a polymer network. The crosslinks make the hydrogel swell-resistant but brittle. This conflict is resolved here by making a hydrogel from a dough. The dough is formed by mixing long polymer chains with a small amount of water and photoinitiator. The dough is then homogenized by kneading and annealing at elevated temperatures, during which the crowded polymer chains densely entangle. The polymer chains are then sparsely crosslinked into a polymer network under an ultraviolet lamp, and submerged in water to swell to equilibrium. The resulting hydrogel is both swell-resistant and tough. The hydrogel also has near-perfect elasticity, high strength, high fatigue resistance, and low friction. The method is demonstrated with two widely used polymers, poly(ethylene glycol) and cellulose. These hydrogels have never been made swell-resistant, elastic, and tough before. The method is generally applicable to synthetic and natural polymers, and is compatible with industrial processing technologies, opening doors to the development of sustainable, high-performance hydrogels.

1. Introduction

Many hydrogels are fabricated from preexisting polymers for two reasons. First, some synthetic polymers, such as poly(ethylene glycol) (PEG),^[1] poly(vinylpyrrolidone) (PVP),^[2] and poly(vinyl alcohol) (PVA),^[3,4] are polymerized under specialized conditions. Second, many sustainable polymers under development are derived from natural polymers, such as cellulose, alginate, chitosan, hyaluronic acid, collagen, and gelatin.^[5]

In the presence of water, some polymers gel by physical bonds, and others gel by chemical crosslinks. The two classes of hydrogels—called physical hydrogels and chemical hydrogels—are illustrated, respectively, by PVA and PEG. Both have excellent biocompatibility and are widely used in bioengineering.^[6] PVA hydrogels form crystalline domains through hydrogen

bonds.^[3] The physical hydrogels resist excessive swell, and have a high load-bearing capacity, characterized by high stiffness, strength, toughness, and fatigue resistance.^[7–10] During deformation, the hydrogen bonds break and reform, so PVA hydrogels exhibit pronounced inelasticity. By contrast, dry PEG crystallizes, but dissolves in water.^[11] To resist excessive swell in water, the chemical hydrogels have dense chemical crosslinks,^[12–14] which embrittle the hydrogels.^[15–20] Slide-ring hydrogels can equalize tension along polymer chains and are highly stretchable and elastic.^[21] However, slide-ring hydrogels reported so far are soft and brittle.^[22] Slide-ring PEG hydrogels with high polymer contents toughen by strain-induced crystallization,^[23] but such hydrogels suffer pronounced swelling due to the low density of slide rings, leading to low stiffness and low toughness in water.^[21,24]

This conflict between swell resistance and toughness originates from the conventional method of fabrication (Figure 1a). Most PEG hydrogels have been synthesized by using crosslinkable PEG derivatives, such as poly(ethylene glycol) diacrylate (PEGDA)^[12] and tetra-arm PEG.^[25] To resist excessive swell, polymers of relatively low molecular weights are commonly used. The short polymer chains are mixed with a large amount of water to form a homogeneous solution. The polymer chains are crosslinked into a polymer network, which is then submerged in water to swell to equilibrium. The resulting hydrogel forms a net-like topology: the polymers are densely crosslinked and sparsely entangled. When the hydrogel is stretched, before a chain breaks, tension is distributed over its short length and to a few other chains through two crosslinks. When a single covalent bond breaks, the energy stored in these few short chains dissipates, resulting in brittleness.^[16,26]

Here we report a method of using pre-existing polymer chains to fabricate chemical hydrogels of both high swell resistance and toughness (Figure 1b). We make a dough by mixing PEG chains of high molecular weights with a small amount of water and photoinitiator. We homogenize the dough by kneading and annealing at elevated temperatures, during which the crowded, long polymer chains densely entangle. We then shine ultraviolet light to sparsely crosslink the polymer chains into a polymer network. The dough is submerged in water to swell to equilibrium. The resulting hydrogel forms a fabric-like topology: the dense entanglements weave and the sparse crosslinks fasten. A polymer network of a topology in which entanglements greatly outnumber crosslinks may be called a tanglemer.

G. Nian, J. Kim, X. Bao, Z. Suo
John A. Paulson School of Engineering and Applied Sciences
Kavli Institute for Bionano Science and Technology
Harvard University
Cambridge, MA 02138, USA
E-mail: suo@seas.harvard.edu

X. Bao
Centre for Polymer from Renewable Resource
SFSE
South China University of Technology
Guangzhou 510640, China

 The ORCID identification number(s) for the author(s) of this article can be found under <https://doi.org/10.1002/adma.202206577>.

DOI: 10.1002/adma.202206577

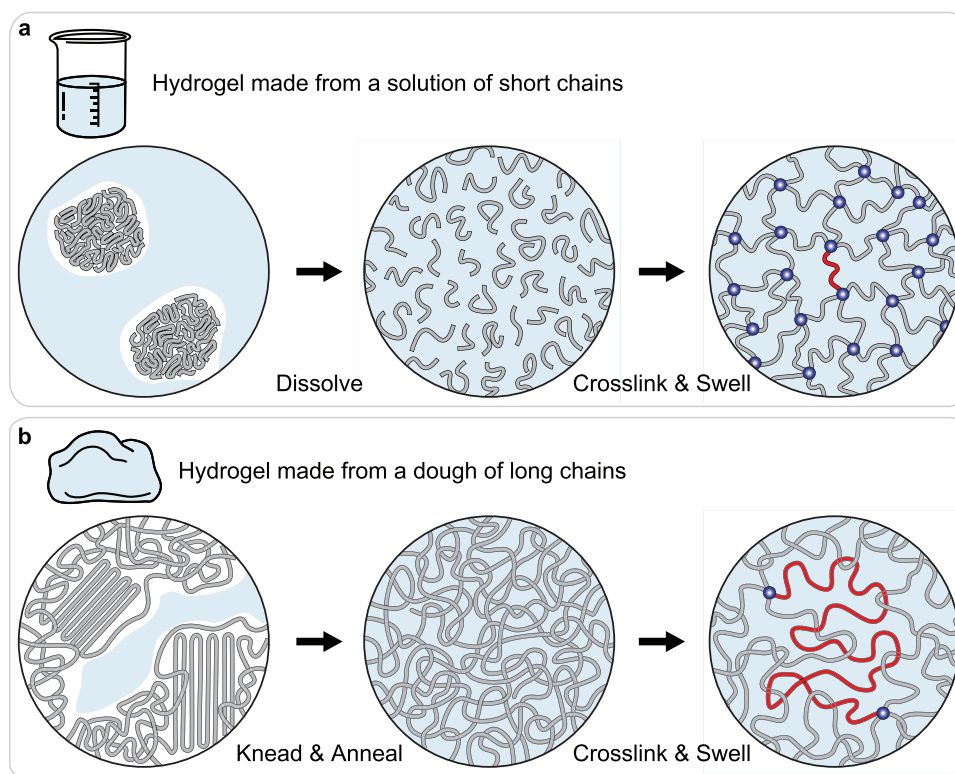


Figure 1. Making hydrogels from preexisting polymers in two ways. a) Make a hydrogel from a solution of short chains: dissolve short polymers in a large amount of water, crosslink the polymers into a network, and swell the network in water to equilibrium. b) Make a hydrogel from a dough of long polymers: mix long polymers with a small amount of water, knead and anneal the mixture to form a homogenized dough, crosslink the polymers into a network, and swell the network in water to equilibrium.

Whereas how entanglements affect the stiffness of polymer networks and the rheology of polymer solutions have long been studied,^[27,28] how entanglements affect the fracture of polymer networks has received attention only recently.^[29,30] When a highly entangled hydrogel is stretched, before a chain breaks, tension is distributed along the long length of the chain and to many chains through entanglements, as well as to a few other chains through two crosslinks.^[30] When a single covalent bond breaks, the energy stored in many long chains dissipates, leading to high toughness. A polymer network in which entanglements greatly outnumber crosslinks resolves the conflict between swell resistance and toughness. The dense entanglements restrain swelling but do not embrittle the polymer network. The sparse crosslinks enable long polymer chains and toughen the polymer network. So far highly entangled hydrogels have been synthesized from the polymerization of monomers.^[29,30] As noted above, existing hydrogels made from preexisting polymers and chemical crosslinks have poor mechanical properties. Consequently, a method to enhance the mechanical properties of such hydrogels will advance technology in terms of biocompatibility, sustainability, and cost-efficiency.

2. Results and Discussion

We synthesize a highly entangled hydrogel from PEG of an ultra-high molecular weight of $8 \times 10^6 \text{ g mol}^{-1}$. We mix the

powder of the PEG polymer chains with unusually small amounts of water and photoinitiator, forming an inhomogeneous and opaque dough (Figure S1, Supporting Information). Let ϕ_1 be the mass ratio of polymer to the dough. A cycle of kneading consists of folding the dough twice, pressing it using aluminum plates to the original thickness in 2 min, and holding the aluminum plates for 9 min, all at 80°C (Figure 2a). After seven cycles of kneading, the dough becomes homogeneous and transparent (Figure 2b). The dough is then annealed at 65°C overnight. The microstructure of the dough is coarse before kneading, refined after seven cycles of kneading, and further refined after annealing (Figure S2, Supporting Information). That the dough becomes transparent after kneading and annealing indicates that polymers are uniformly distributed in the nanoscale (Figure S3, Supporting Information). In a rheometer, the dough behaves like a viscous liquid at a low frequency, and like an elastic solid at a high frequency (Figure 2c). The rheology of the dough quantifies the state of entanglement. Following a common practice, we use the plateau modulus to calculate the entanglement molecular weight M_e (Note S1, Supporting Information), and find that it scales as $M_e \sim \phi_1^{-4/3}$ (Figure 2d). The scaling is commonly observed in highly entangled polymer solutions.^[31] At $\phi_1 = 0.75$, $M_e = 4.5 \times 10^3 \text{ g mol}^{-1}$ is much lower than the molecular weight of the as-received polymer ($8 \times 10^6 \text{ g mol}^{-1}$), giving ≈ 1800 entanglements per polymer chain. Furthermore, by extrapolation of the experimental data in Figure 2d, we estimate that the entanglement

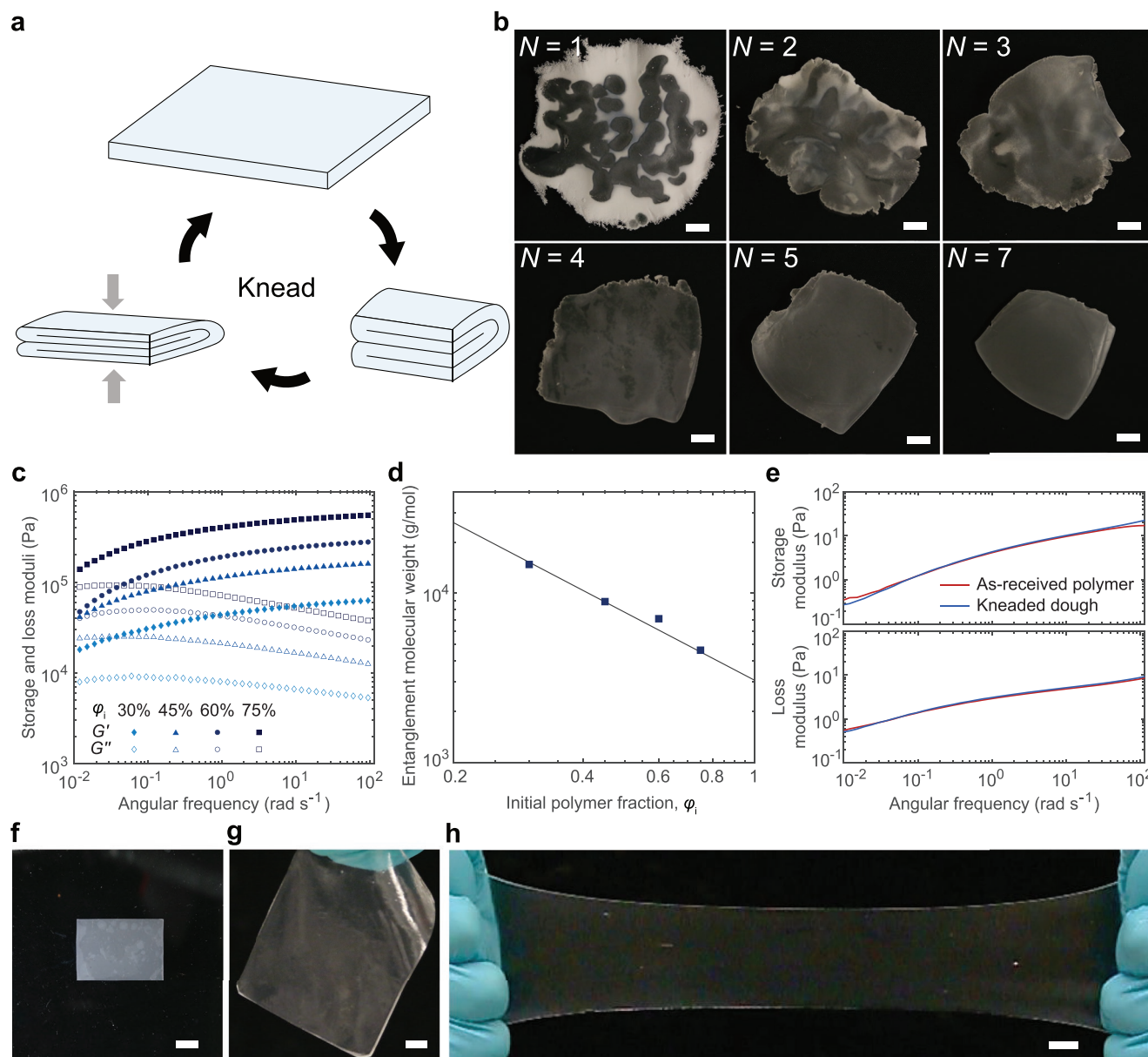


Figure 2. Making a highly entangled hydrogel through a dough. Make a dough by mixing a powder of long-chain PEG with small amounts of water and benzophenone. a) The dough is homogenized by kneading at an elevated temperature. b) The dough ($\phi_i = 75\%$) becomes homogeneous in seven cycles of kneading. c) The storage and loss moduli as functions of frequency for doughs after kneading. d) The entanglement molecular weight of doughs as a function of ϕ_i . e) Storage and loss moduli of a solution of as-received polymer are compared to those of a solution of kneaded dough. Each solution contains 1% of polymer in mass. f) The dough is then annealed at 65 °C overnight, and crosslinked under ultraviolet light. g) The crosslinked dough is submerged in water to swell to equilibrium. h) The resulting hydrogel is transparent and highly stretchable. Scale bars: 1 cm.

molecular weight for the polymer without water is $\approx 2600 \text{ g mol}^{-1}$. This value is close to the reported entanglement molecular weight of PEG melt, $\approx 2200 \text{ g mol}^{-1}$.^[32] This comparison indicates that, after the dough is annealed, the entanglements have reached equilibrium. For all frequencies tested, the solution of as-received polymer and the solution of kneaded dough have comparable moduli (Figure 2e). This finding confirms that kneading causes the scission of polymer chains negligibly. When the dough is placed under an ultraviolet lamp, the benzophenone molecules are activated, abstract hydrogen atoms from PEG chains, and create radicals along the chains. When

two radicals encounter, they form a crosslink (Figure 2f and Figure S4, Supporting Information). The crosslinked dough is then submerged in water to swell to equilibrium (Figure 2g). The resulting hydrogel is transparent, elastic, stretchable, and tough (Figure 2h and Video S1, Supporting Information).

The kneading and annealing of polymers, with or without solvent, have long been used to process elastomers and food, but have so far not been used to process hydrogels. On the basis of the physics and chemistry of PEG, we design the process such that polymer chains do not degrade or break, but densely entangle. Dry PEG is semicrystalline, which melts at $\approx 65 \text{ °C}$. It

dissolves in a large amount of water at room temperature. The dry powder, as well as powder mixed with a small amount of water, remains powdery after being kept at an elevated temperature overnight (Figures S5 and S6, Supporting Information). However, PEG degrades substantially when kept at elevated temperature for too long.^[33] Mixing the powder with a small amount of water lowers viscosity and eases homogenization, but mixing the powder with too much water makes the polymer chains slightly entangled. The mixture must be kneaded at a slow rate to avoid breaking the long polymer chains. The PEG with a small amount of water remains powdery after kneading at room temperature (Video S2, Supporting Information), but turns into a homogeneous dough after kneading at elevated temperature. Right after kneading, the polymer chains are in an extended, nonequilibrium state. During annealing, the polymer chains coil and entangle by thermal motion, approaching equilibrium. Annealing temperature should not be lower than the melting point of PEG, and should not be too high to cause thermal degradation. Guided by these observations, we mix the as-received polymer with suitable amounts of water and photoinitiator, knead the dough in a window of temperature, number of cycles, and rate of deformation, and anneal the dough in a window of temperature and time.

To contrast the net-like topology and fabric-like topology, we prepare a conventional short-chain hydrogel using PEGDA of molecular weight of $7 \times 10^2 \text{ g mol}^{-1}$ (Figure S7, Supporting

Information), and a highly entangled hydrogel using PEG chains of molecular weight of $8 \times 10^6 \text{ g mol}^{-1}$. We compare the two types of hydrogels through various tests. We glue the two hydrogels to acrylic rings and puncture them using a glass rod. The short-chain hydrogel punctures at a small displacement and cracks emanate from the punctured hole (Figure 3a and Video S3, Supporting Information). The highly entangled hydrogel punctures at a large displacement (9.4 times greater than that of the short-chain hydrogel), and no cracks emanate from the punctured hole (Figure 3b and Video S4, Supporting Information). We then cut sheets of the two hydrogels into dogbone-shaped samples, and stretch them using a tensile tester. The two hydrogels have remarkably different stress–stretch curves (Figure 3c). The highly entangled hydrogel has a lower final polymer fraction and stiffness than the short-chain hydrogel, but has higher toughness, fatigue threshold, extensibility, work of fracture, and tensile strength than the short-chain hydrogel (Figure 3d and Figure S8, Supporting Information). Toughness and work of fracture have different units, J m^{-2} and J m^{-3} . Their ratio defines a material-specific length.^[34] The ratio of our measured toughness and work of fracture gives the length 1.8 mm. When flaws in the material are smaller than this material-specific length, the material is flaw insensitive. We also cut two hydrogels into disks, and measure the compressive strengths. The highly entangled hydrogel has about 5.2 times higher compressive strength than

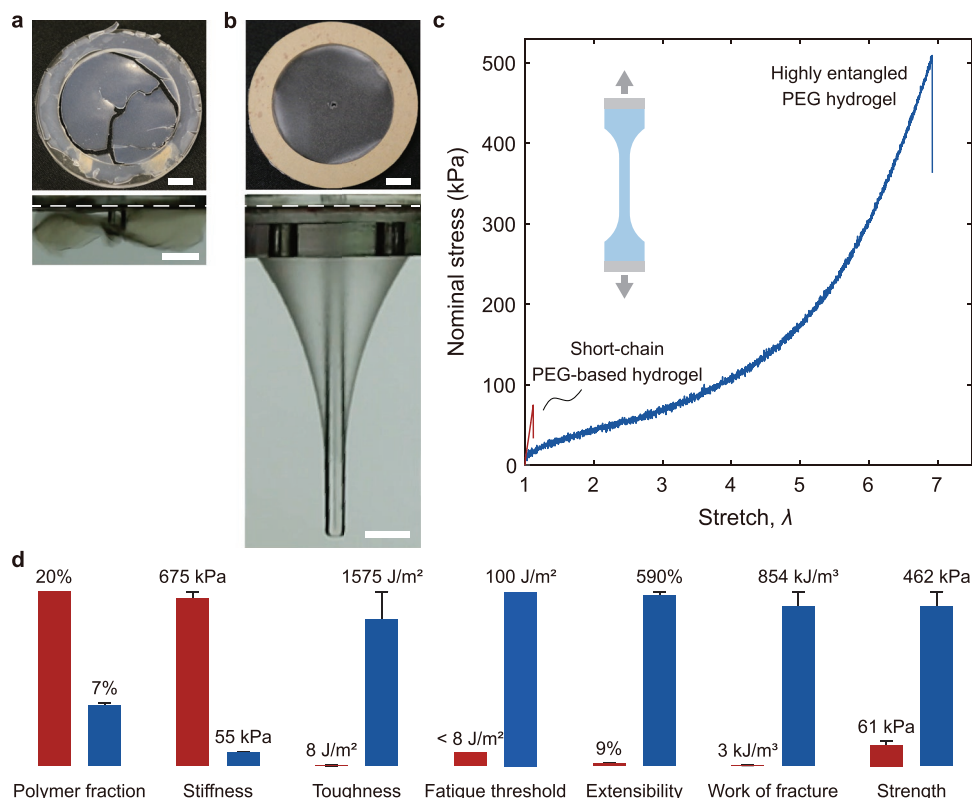


Figure 3. Comparison of a short-chain PEG-based hydrogel and a highly entangled PEG hydrogel. a) The short-chain hydrogel punctures at a small displacement, with cracks emanating from the punctured hole. b) The highly entangled hydrogel punctures at a large displacement, with no cracks emanating from the punctured hole. The white dashed lines indicate the positions of the two undeformed hydrogels. Scale bars: 1 cm. c) The stress–stretch curves of the two hydrogels. d) The highly entangled hydrogel (blue columns) differs from the short-chain hydrogel (red columns) in various properties.

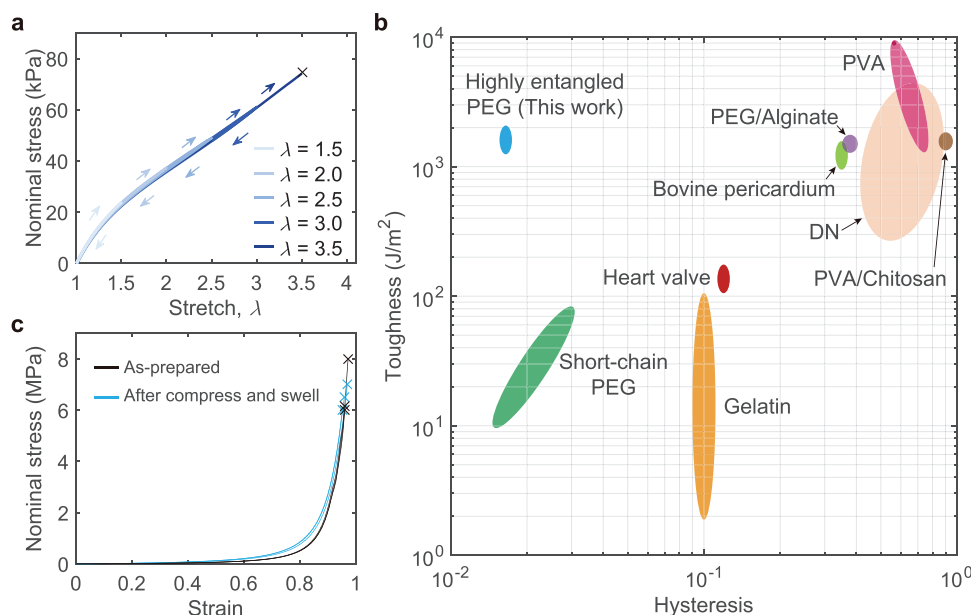


Figure 4. Highly entangled PEG hydrogels are elastic and tough. a) A highly entangled PEG hydrogel exhibits near-perfect elasticity with negligible hysteresis. b) Highly entangled PEG hydrogels are compared with existing hydrogels on the toughness-hysteresis plane.^[8,16,39,41–51] c) Two types of experiments are conducted on the highly entangled hydrogel. First, the hydrogel is compressed to rupture. Second, the hydrogel is compressed ten times to a pressure of 4 MPa, submerged in water to swell to equilibrium, and then compressed to rupture. Each experiment is repeated three times.

the short-chain hydrogel (Figure S9 and Videos S5 and S6, Supporting Information).

The highly entangled PEG hydrogel has a friction coefficient of 0.028, and the short-chain PEG-based hydrogel has a friction coefficient of 0.55 (Figure S10, Supporting Information). This marked difference is understood as follows. On the surface of the hydrogels, hydrophilic polymer chains stabilize a layer of water, which lubricates the surface.^[35,36] The friction decreases as the thickness of the layer increases, and the thickness increases as the length of polymer chains increases. The long length of polymer chains of the highly entangled hydrogel gives a low friction coefficient.

The highly entangled hydrogel exhibits near-perfect elasticity: the stress–stretch curves have negligible hysteresis (Figure 4a) and are insensitive to the rate of stretch (Figure S11, Supporting Information). The near-perfect elasticity results from two facts. First, the large amount of water in the swollen hydrogel reduces interchain friction. By comparison, the crosslinked dough exhibits pronounced hysteresis (Figure S12, Supporting Information). Second, the highly entangled hydrogels have no sacrificial bonds. By comparison, when a double network (DN) hydrogel is stretched, a short-chain network breaks while a long-chain network is intact, leading to high hysteresis.^[37] Sacrificial bonds and high hysteresis are common in many hydrogels, including alginate–polyacrylamide (PAAm) hydrogel^[38] and PVA hydrogel.^[8,9,39]

It has been suggested that viscoelasticity due to slip of entanglements toughens hydrogels.^[29] By contrast, we find that, due to the low viscosity of water, entanglements in swollen hydrogels readily slip and negligibly dissipate energy before rupture. Indeed, this ease of slip is a prerequisite for tension to de-concentrate along long chains and leads to high toughness. The high toughness with near-perfect elasticity supports our understanding of the role of entanglements.

In most hydrogels, hysteresis and toughness are positively correlated. They measure energy dissipation in two tests. Hysteresis measures energy dissipated in loading and unloading a sample without crack propagation. Toughness measures energy dissipated in crack propagation. Indeed, such hysteresis–toughness correlation has been commonly stated as a design principle in developing tough hydrogels.^[37,38,40] The DN hydrogel, alginate–PAAm hydrogel, and PVA hydrogel all have both high hysteresis and high toughness, whereas the short-chain PEG-based hydrogel has low hysteresis and low toughness (Figure 4b). The highly entangled hydrogel is exceptional in that it breaks the hysteresis–toughness correlation and simultaneously achieves low hysteresis and high toughness. The highly entangled hydrogel achieves high toughness not by sacrificial bonds, but by having all chains long.

Furthermore, a high toughness with near-perfect elasticity allows the highly entangled hydrogel to resist fatigue. Under cyclic loading, sacrificial bonds and viscoelasticity do not enhance the fatigue threshold,^[29,52] whereas the de-concentration of tension does.^[46,53] As we have shown in Figure 3d, the highly entangled PEG hydrogel has a much higher fatigue threshold than short-chain PEG-based hydrogels, as well as fully swollen tetra-arm PEG hydrogels.^[54] The high fatigue threshold and low hysteresis support that the entanglements slip easily and de-concentrate tension.

In a hydrogel with sacrificial bonds, upon loading, the sacrificial bonds break and normally do not heal within a short time. Consequently, the hydrogel degrades and has a different stress–stretch curve upon reloading.^[38,55] Submerged in water, the degraded hydrogel swells more and becomes even weaker. These shortcomings do not appear in a highly entangled hydrogel. We conduct two types of experiments (Figure 4c). First, we compress a sample to rupture. Second, we compress

a sample ten times to a pressure of 4 MPa, swell it in water overnight, and then compress it to rupture. We perform each type of experiment on three samples and find that the strength varies from sample to sample, but the average strengths measured in the two types of experiments are the same, ≈ 6.5 MPa. Also, the stress–strain curves of the two types of experiments only differ slightly. These findings confirm that the highly entangled hydrogel degrades negligibly under repeated load.

The properties of hydrogels made from doughs depend on various synthesis parameters, including the initial polymer fraction ϕ_i , the benzophenone ratio B (the molar ratio of benzophenone to monomer unit of the polymer), and molecular weight of the polymer M_v . Each dough is homogenized and crosslinked, and then submerged in water to form an equilibrium hydrogel. When B , ϕ_i , and M_v are low, the dough dissolves in water. When B , ϕ_i , and M_v exceed critical conditions, the dough gels and swells to equilibrium. In either case, let ϕ_f be the final mass fraction of polymer in the equilibrated sample. We plot the final polymer fraction ϕ_f for samples made of PEG of molecular weight $M_v = 8 \times 10^6$ g mol $^{-1}$ and various values of B and ϕ_i (Figure 5a). At fixed values of ϕ_i and M_v , a critical value of B exists, below which the dough dissolves, so that ϕ_f is low, set by the mass ratio of the polymers and water in the container. The critical B decreases as ϕ_i increases. Above the critical value of B , the dough swells to an equilibrium hydrogel. At any B , the higher the polymer fraction in the dough, ϕ_i , the higher the

polymer fraction in the equilibrium hydrogel, ϕ_f . These observations support the molecular interpretation that the entanglements and the crosslinks together maintain the topology of the polymers in a hydrogel. The higher the initial polymer fraction ϕ_i , the more crowded the polymers in a dough, and the denser the entanglements. A highly entangled dough ($\phi_i = 75\%$ and $B = 3.2 \times 10^{-4}$) swells by about a factor of ten, as calculated from the observed equilibrium polymer fraction. This amount of swelling is unsurprising because the dough is concentrated with PEG, which is hydrophilic. The entanglements are not dense enough even in a dough of highly entangled polymer network to prevent swelling. However, hydrogels of sparse entanglements ($\phi_i < 75\%$ and $B = 3.2 \times 10^{-4}$) swell much more than a factor of ten.

This molecular interpretation is corroborated by elastic modulus E of the equilibrium hydrogels plotted as a function of B and ϕ_i at $M_v = 8 \times 10^6$ g mol $^{-1}$ (Figure 5b). At $B = 1 \times 10^{-3}$, the hydrogel made of a dough of $\phi_i = 75\%$ has a modulus $E \approx 30$ times higher than the hydrogel made of a dough of $\phi_i = 45\%$, and the hydrogel made of a dough of $\phi_i = 30\%$ has negligible modulus. We also measure toughness Γ of equilibrium hydrogel as a function of B and ϕ_i at $M_v = 8 \times 10^6$ g mol $^{-1}$ (Figure 5c). As B decreases, the crosslink density decreases, and the toughness increases. This trend is consistent with the prediction of the Lake–Thomas model.^[52] When $\phi_i = 60\%$, the critical value of B is 3.2×10^{-4} , and a low crosslink density gives

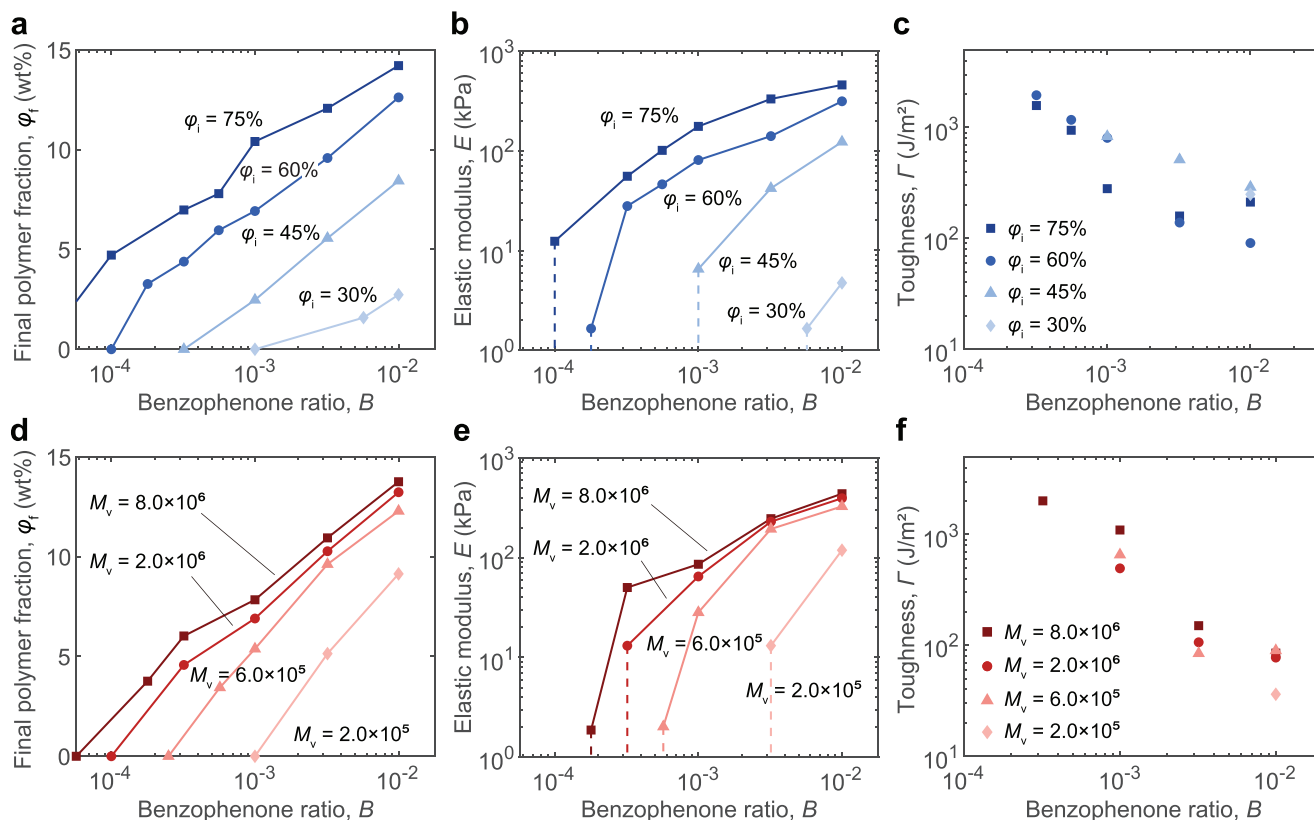


Figure 5. The properties of hydrogels made from doughs of long-chain PEG depend on various synthesis parameters. a) The final polymer fraction ϕ_f as a function of the benzophenone ratio B at different initial polymer fraction ϕ_i . b) The elastic modulus E as a function of B at different ϕ_i . c) The toughness Γ as a function of B at different ϕ_i . d) ϕ_f as a function of B at different molecular weights M_v . e) E as a function of B at different M_v . f) Γ as a function of B at different M_v .

a high toughness of 2000 J m^{-2} . When $\phi_1 = 30\%$, the critical value of B is 1×10^{-2} , and a high crosslink density gives a toughness of only 250 J m^{-2} . We have also tried $\phi_1 = 100\%$ but the resulting hydrogel remains inhomogeneous after the kneading process used in lower values of ϕ_1 (Figure S13, Supporting Information).

We next characterize equilibrium hydrogels made from doughs of PEG chains of various molecular weights, crosslinked using various amounts of benzophenone. All these doughs are prepared at the same initial polymer fraction, $\phi_1 = 65\%$. Again, at fixed values of ϕ_1 and M_v , a critical value of B exists below which the dough dissolves in water so that ϕ_f is low (Figure 5d). The critical B decreases as M_v increases. Also, at any B , a higher M_v gives a higher ϕ_f . These observations indicate that a hydrogel made of polymers of a higher molecular weight has denser entanglements. Also, as M_v increases, ϕ_f increases rapidly when M_v is low and increases slowly when M_v is high. We interpret this behavior as follows. In the crosslinked network, the two ends of a polymer chain are dangling. Consequently, a portion of the chain at each end can detangle under stress, and does not contribute to swell resistance. When M_v is low, the portion of dangling chains is high, resulting in lower ϕ_f . When M_v is high enough, the portion of dangling chains is negligible, so that ϕ_f is insensitive to the molecular weight. This molecular interpretation is corroborated in elastic modulus (Figure 5e). For example, at $B = 3.2 \times 10^{-4}$, the moduli of the hydrogels made from polymers of $M_v > 6 \times 10^5$ are on the order of 10 kPa, whereas the moduli of the hydrogels made from polymers of $M_v < 6 \times 10^5$ are vanishingly low. We plot the toughness of equilibrium hydrogels (Figure 5f). The toughness is not sensitive to M_v , but the high value of M_v enables polymers to have low values of B and high toughness. This observation is consistent with the Lake-Thomas prediction that the toughness depends on the polymer chain length between crosslinks. We compare the stress–stretch curves of some of the conditions in Figure 5 to the theory of elasticity of entangled networks (Figures S14–S16 and Note S2, Supporting Information). We also compare the swelling ratio to the theory of elasticity of gels (Note S3, Supporting Information). We have measured the mechanical properties of hydrogels made with doughs annealed at various temperatures for various times (Figure S17, Supporting Information). For a given annealing temperature, the mechanical properties of hydrogels plateau after some time. This observation indicates that the entanglements reach equilibrium after a dough is annealed at a temperature for a sufficient time.

In classic models of networks without entanglements, stiffness, stretchability, and fatigue threshold are related to the number of monomers per chain (Note S4 and Figure S18, Supporting Information). Using these models and measured values of the three material properties, we estimate three values of the number of monomers per chain, 1016, 357, and 37 467, respectively. We interpret the large difference between the third estimate and the first two to the presence of dense entanglements. Compared to a network without entanglements, a highly entangled network increases stiffness and decreases stretchability, because the entangled chains cannot pass one another without scission. Entanglements, however, do not affect the fatigue threshold, because the entangled chains slip readily and de-concentrate tension over entire chains. Both stiffness

and stretchability can be used to define the effective density of entanglements, but the two definitions lead to somewhat different values, as indicated by the above numbers.

Strain-induced crystallization has been shown to toughen slide-ring PEG hydrogels, where the polymer fraction is above 20%.^[23] We confirm strain-induced crystallization for our hydrogels when the polymer fraction is 20%, but do not observe strain-induced crystallization in fully swollen hydrogels, in which polymer fraction is 7% (Figure S19, Supporting Information). Thus, our hydrogel attains high toughness through stress de-concentration of densely entangled long polymer chains, rather than strain-induced crystallization.

Our method has the potential to develop sustainable hydrogels using polymers derived from abundant natural products. To illustrate, we synthesize highly entangled hydrogels using long-chain 2-hydroxyethyl cellulose. The 2-hydroxyethyl cellulose is modified from naturally existing cellulose, forms fewer hydrogen bonds than native cellulose, and dissolves in water.^[56] We prepare a dough of long-chain 2-hydroxyethyl cellulose ($M_v \approx 1.3 \times 10^6 \text{ g mol}^{-1}$), homogenize the dough by kneading at 80°C , crosslink the dough using glycidyl methacrylate (GMA)^[57] and Irgacure 2959, and swell the dough in water to form an equilibrium hydrogel (Figure S20, Supporting Information). The equilibrium hydrogel has the polymer fraction $\phi_f = 20\%$, is transparent (Figure 6a), and achieves excellent mechanical properties (Figure 6b). The modulus is 200 kPa, the strength is 642 kPa, and the toughness is 200 J m^{-2} . The highly entangled cellulose hydrogel also exhibits near-perfect elasticity: the hysteresis is negligible (Figure 6c), and the stress–stretch curve is rate-insensitive (Figure 6d). Such a combination of material properties is distinctive, given that existing swell-resistant and strong cellulose hydrogels have large hysteresis.^[58]

For each type of polymer, one should ensure long polymer chains are available, and frictional interaction between polymer chains is weak. To densely entangle polymer chains while avoiding breaking them, one should design the process conditions, including the temperature, strain rate, and the number of cycles for kneading, as well as temperature and time for annealing.

Recall that elastomers are commonly processed by kneading without solvents. Such a process usually breaks long polymers, and is commonly called mastication.^[59] Mastication lowers viscosity and eases the process. The elastomer made this way has relatively short chains and low fatigue resistance. It is conceivable that, under suitable conditions, kneading and annealing with or without solvent can process elastomers of high molecular weights without scission and with dense entanglements, achieving superior mechanical properties.

3. Conclusion

We report a method of using preexisting polymer chains to fabricate a chemical hydrogel from a dough. The dough is formed by mixing the polymer chains of high molecular weights with a small amount of water and photoinitiator. Kneading and annealing homogenize the dough and entangle the polymer chains without breaking them. Under ultraviolet light, polymer chains crosslink into a polymer network, which is then

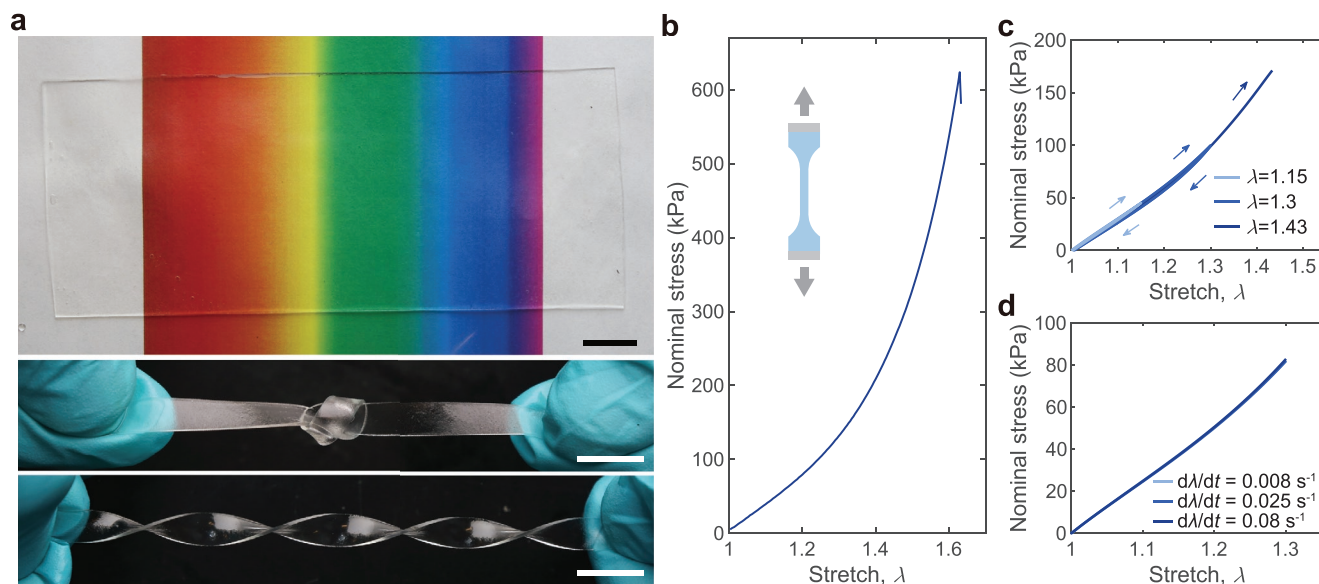


Figure 6. Highly entangled cellulose hydrogels. a) The hydrogel is transparent and can be knotted and twisted. Scale bars are 1 cm. b) Stress–stretch curve up to fracture. c) Near-perfect elasticity with negligible hysteresis. d) Rate-insensitive stress–stretch curves.

submerged in water to swell to equilibrium. Such a hydrogel resolves the conflict between swell resistance and toughness while having near-perfect elasticity. Our method is generally applicable to synthetic and natural polymers, and is compatible with industrial processing technologies, opening doors to the development of sustainable, high-performance hydrogels.

4. Experimental Section

Materials: Polyethylene glycol (PEG, $M_v = 2 \times 10^5 \text{ g mol}^{-1}$, $6 \times 10^5 \text{ g mol}^{-1}$, $2 \times 10^6 \text{ g mol}^{-1}$, and $8 \times 10^6 \text{ g mol}^{-1}$), polyethylene glycol diacrylate (PEGDA, $M_n = 700 \text{ g mol}^{-1}$), 2-hydroxyethyl cellulose ($M_v = 1.3 \times 10^6 \text{ g mol}^{-1}$), benzophenone, glycidyl methacrylate (GMA), Irgacure 2959, and hydrochloric acid (HCl, 37%) were purchased from Sigma-Aldrich and used without further purification. Isopropyl alcohol (IPA) was purchased from VWR. Distilled water was purchased from Poland Spring.

Preparation of Highly Entangled PEG Hydrogels: The highly entangled PEG hydrogels were prepared in the following steps: mix, knead, anneal, crosslink, and swell. As the amount of benzophenone was small, it was first dissolved in 1.2 g of IPA, and then mixed 2.5 g of PEG powder with the benzophenone solution by stirring for 2 min. The mixture was left in an oven at 65 °C for 15 min to evaporate the IPA. Then powders of PEG and benzophenone were mixed roughly with water to form a dough. The dough was initially inhomogeneous. To homogenize the dough, it was kneaded at an elevated temperature. The dough was placed between a pair of aluminum plates (McMaster-Carr 1655T8) with a 0.5 mm-thick polyethylene spacer, compressed by using eight C-shaped clamps (McMaster-Carr 5133A13) in 2 min, and held for nine min, all at 80 °C in the oven. The dough slowly became a thin film with the thickness of the spacer. Then, the dough was folded twice, once horizontally and once vertically. Folding twice and compressing it in the oven constituted a cycle of kneading. Water molecules evaporated somewhat during kneading (Figure S21, Supporting Information). After seven cycles of kneading, the dough was annealed in the oven for 12 h at 65 °C. The homogenized dough was crosslinked for 1.3 h under ultraviolet light ($\approx 11 \text{ mW cm}^{-2}$, 365 nm) in a nitrogen environment. During kneading, annealing, and crosslinking, the dough was kept in a plastic bag (reclosable zip bag, VWR) to prevent drying. The crosslinked dough was swelled in water for one day to reach equilibrium. The highly entangled

PEG hydrogel used in Figure 2, Figure 3, and Figure 4 was synthesized from a dough with an initial polymer fraction $\phi_i = 75\%$, molecular weight $M_v = 8 \times 10^6 \text{ g mol}^{-1}$, and benzophenone ratio $B = 3.2 \times 10^{-4}$.

Preparation of Short-Chain PEG-Based Hydrogel: The short-chain PEG-based hydrogel was prepared by using PEGDA. A precursor was prepared consisting of 20 wt% of PEGDA, 0.02 wt.% of Irgacure 2959, and water. The precursor was poured into a glass mold and cured for 6 h under ultraviolet light.

Preparation of Highly Entangled Cellulose Hydrogels: An HCl solution was prepared with pH value of 3.5. 0.1 mL of GMA and 20 mg of Irgacure 2959 were dissolved in 3 mL of HCl solution. The solution and 2 g of 2-hydroxyethyl cellulose were mixed, and rest it at 25 °C for 1 h to obtain a cellulose dough. The dough was compressed by using a pair of aluminum plates, a 0.5 mm-thick polyethylene spacer, and eight C-shaped clamps, and stored in an oven at 80 °C for 15 min. Then, the dough was annealed at 50 °C for 24 h. After annealing, it was cured for 20 min under ultraviolet light. During all processes, the dough was kept in a plastic bag to prevent drying. Before any measurement, the hydrogels were swelled in water for one day to reach equilibrium.

Measurement of Storage and Loss Moduli of Doughs: The plateau modulus of PEG doughs with different polymer fractions was measured by using a rheometer (DHR-3, TA Instruments). The dough was prepared without cross-linking. As-prepared doughs were cut into dish-like samples with a diameter of 20 mm, and a flat steel plate of the same diameter was adopted. Before each test, the sample was held under compression at 80 °C for 30 min. Paraffin oil was applied at the edge of the sample to prevent evaporation. Samples were measured over a range of oscillation frequencies at a constant oscillation amplitude of 1% and temperature of 80 °C.

Characterization of Polymer Scission: Two aqueous solutions of PEG were compared. One was prepared by dissolving as-received PEG powder in water, and the other was by dissolving the kneaded PEG dough in water. As the molecular weight ($M_v = 8 \times 10^6 \text{ g mol}^{-1}$) is ultra-high, to ease the process of dissolving, a low polymer fraction of 1% in mass was used. The property of each solution was characterized by measuring the storage and loss moduli by using the rheometer. A cone plate with a cone angle of 2° and a diameter of 60 mm was used. Each solution was measured over a range of oscillation frequencies at a constant oscillation amplitude of 1% and temperature of 25 °C.

Measurements of Material Properties: The final polymer fraction ϕ_f is the ratio of the weight of the polymer powder to the weight of the

equilibrium hydrogel. The elastic modulus E , toughness Γ , hysteresis, rate-sensitivity, and fatigue threshold were measured using pure-shear tests. The dimensions of each sample were $89\text{ mm} \times 12.7\text{ mm} \times \approx 1\text{ mm}$ (width \times height \times thickness). The samples were glued to grippers made of an acrylic sheet by using Krazy glue. The elastic modulus was calculated from an initial slope of a stress–stretch curve, by $0.75ds/d\lambda$, where s is the nominal stress and λ is the stretch. To measure the toughness, an unnotched sample was stretched to obtain the elastic energy per unit volume, $W(\lambda)$, a notched sample (the length of the precrack is 20 mm) was stretched until fracture to get the critical stretch λ_c , and the toughness was calculated by $\Gamma = HW(\lambda_c)$, where H is the height of the undeformed sample. Hysteresis was measured by cyclic loading. The area below the loading curve A_{loading} and the area below the unloading curve $A_{\text{unloading}}$ were calculated. The hysteresis was calculated as $1 - A_{\text{unloading}}/A_{\text{loading}}$. For the rate-sensitivity, a cyclic stretch was applied with a stretch of 2 at various loading rates, and stress–stretch curves were measured. The stretch rate was 0.016 s^{-1} in the above measurements, except for the rate-sensitivity. In the fatigue fracture test, a sharp crack was introduced into a sample, the sample was submerged in water, loading-unloading was applied at a prescribed stretch for 10000 cycles with a frequency of $\approx 1.0\text{ Hz}$, and crack growth was measured using an optical microscope. The energy release rate was calculated by $G = HW(\lambda)$ and dc/dN by dividing the crack growth by the number of cycles. The stress–stretch curve, extensibility, work of fracture, and strength were measured through uniaxial tension tests. An $\approx 1\text{ mm}$ -thick hydrogel sheet was cut into dogbone-shaped samples. The gauge section of each sample had dimensions of $4\text{ mm} \times 20\text{ mm}$ (width \times height). A video was taken during the test to obtain the real extension of the gauge section of each sample. The work of fracture was the area under the stress–stretch curve. The stretch rate was $\approx 0.04\text{ s}^{-1}$. To measure the compressive strength, an $\approx 1\text{ mm}$ -thick hydrogel sheet was cut into coin-shaped samples. The strain rate was $\approx 4.2 \times 10^{-3}\text{ s}^{-1}$. All tests were performed by using a mechanical tester (Instron 5966).

Puncture Test: A hydrogel sheet $\approx 1\text{ mm}$ thick was cut into a circular sample with a diameter of 60 mm . The hydrogel was glued onto a rigid acrylic ring with an inner diameter of 50 mm , by using the Krazy glue. The ring was fixed to a supporter. A glass rod with a diameter of 4.7 mm was clamped by the gripper of the mechanical tester. The glass rod was placed above the middle of the hydrogel, and then moved at a constant speed of 0.2 mm s^{-1} to puncture the hydrogel.

Supporting Information

Supporting Information is available from the Wiley Online Library or from the author.

Acknowledgements

This work was supported by MRSEC (DMR-2011754). J.K. acknowledges financial support from the Kwanjeong Educational Foundation.

Conflict of Interest

The authors declare no conflict of interest.

Authors Contribution

G.N. and J.K. contributed equally to this work. G.N., J.K., and Z.S. designed the study. G.N. developed the synthesis method. G.N., J.K., and X.B. conducted the experiments. G.N., J.K., and Z.S. wrote the manuscript. Z.S. supervised the research. All authors discussed the result and commented on the manuscript.

Data Availability Statement

The data that support the findings of this study are available from the corresponding author upon reasonable request.

Keywords

elasticity, entanglement, hydrogels, poly(ethylene glycol), toughness

Received: July 19, 2022
Revised: September 11, 2022
Published online:

- [1] I. Dimitrov, C. B. Tsvetanov, *Polym. Sci. Compr. Ref.* **2012**, 4, 551.
- [2] F. Haaf, A. Sanner, F. Straub, *Polym. J.* **1985**, 17, 143.
- [3] C. M. Hassan, N. A. Peppas, in *Biopolymers: PVA Hydrogels Anionic Polymers Nanocomposites*, Advances in Polymer Science, Vol. 153, Springer, Berlin/Heidelberg, Germany **2000**, pp. 37–65.
- [4] M. L. Hallensleben, R. Fuss, F. Mummy, in *Ullmann's Encyclopedia of Industrial Chemistry*, Wiley-VCH, Weinheim, Germany **2015**, https://doi.org/10.1002/14356007.a21_743.pub2.
- [5] M. Baumgartner, F. Hartmann, M. Drack, D. Preninger, D. Wirthl, R. Gerstmayr, L. Lehner, G. Mao, R. Pruckner, S. Demchyshyn, L. Reiter, M. Strobel, T. Stockinger, D. Schiller, S. Kimeswenger, F. Greibich, G. Buchberger, E. Bradt, S. Hild, S. Bauer, M. Kaltenbrunner, *Nat. Mater.* **2020**, 19, 1102.
- [6] K. Y. Lee, D. J. Mooney, *Chem. Rev.* **2001**, 101, 1869.
- [7] S. R. Stauffer, N. A. Peppas, *Polymer* **1992**, 33, 3932.
- [8] S. Lin, X. Liu, J. Liu, H. Yuk, H.-C. Loh, G. A. Parada, C. Settens, J. Song, A. Masic, G. H. McKinley, X. Zhao, *Sci. Adv.* **2019**, 5, eaau8528.
- [9] M. Hua, S. Wu, Y. Ma, Y. Zhao, Z. Chen, I. Frenkel, J. Strzalka, H. Zhou, X. Zhu, X. He, *Nature* **2021**, 590, 594.
- [10] F. Yang, J. Zhao, W. J. Koshut, J. Watt, J. C. Riboh, K. Gall, B. J. Wiley, *Adv. Funct. Mater.* **2020**, 30, 2003451.
- [11] J. Herzberger, K. Niederer, H. Pohlitz, J. Seiwert, M. Worm, F. R. Wurm, H. Frey, *Chem. Rev.* **2016**, 116, 2170.
- [12] C.-C. Lin, K. S. Anseth, *Pharm. Res.* **2009**, 26, 631.
- [13] A. J. Vernengo, in *Adhesives - Applications and Properties*, (Ed: A. Rudawska) InTechOpen, London, UK **2016**, pp. 99–136.
- [14] P. J. M. Bouten, M. Zonjee, J. Bender, S. T. K. Yauw, H. van Goor, J. C. M. van Hest, R. Hoogenboom, *Prog. Polym. Sci.* **2014**, 39, 1375.
- [15] Y. Hou, C. A. Schoener, K. R. Regan, D. Munoz-Pinto, M. S. Hahn, M. A. Grunlan, *Biomacromolecules* **2010**, 11, 648.
- [16] J. Cui, M. A. Lackey, A. E. Madkour, E. M. Saffer, D. M. Griffin, S. R. Bhatia, A. J. Crosby, G. N. Tew, *Biomacromolecules* **2012**, 13, 584.
- [17] O. Z. Higa, S. O. Rogero, L. D. B. Machado, M. B. Mathor, A. B. Lugao, *Radiat. Phys. Chem.* **1999**, 55, 705.
- [18] N. A. Peppas, E. W. Merrill, *J. Appl. Polym. Sci.* **1977**, 21, 1763.
- [19] H. J. Kong, E. Wong, D. J. Mooney, *Macromolecules* **2003**, 36, 4582.
- [20] A. Khanlari, J. E. Schulteis, T. C. Suekama, M. S. Detamore, S. H. Gehrke, *J. Appl. Polym. Sci.* **2015**, 132, <https://doi.org/10.1002/app.42009>.
- [21] Y. Okumura, K. Ito, *Adv. Mater.* **2001**, 13, 485.
- [22] L. Jiang, C. Liu, K. Mayumi, K. Kato, H. Yokoyama, K. Ito, *Chem. Mater.* **2018**, 30, 5013.
- [23] C. Liu, N. Morimoto, L. Jiang, S. Kawahara, T. Noritomi, H. Yokoyama, K. Mayumi, K. Ito, *Science* **2021**, 372, 1078.
- [24] T. Karino, M. Shibayama, K. Ito, *Phys. B (Amsterdam, Neth.)* **2006**, 385–386, 692.

- [25] T. Sakai, T. Matsunaga, Y. Yamamoto, C. Ito, R. Yoshida, S. Suzuki, N. Sasaki, M. Shibayama, U.-i. Chung, *Macromolecules* **2008**, *41*, 5379.
- [26] Y. Akagi, H. Sakurai, J. P. Gong, U.-i. Chung, T. Sakai, *J. Chem. Phys.* **2013**, *139*, 144905.
- [27] P. J. Flory, *Principles of Polymer Chemistry*, Cornell University Press, Ithaca, NY, USA **1953**.
- [28] P. G. de Gennes, *J. Chem. Phys.* **1971**, *55*, 572.
- [29] C. Norioka, Y. Inamoto, C. Hajime, A. Kawamura, T. Miyata, *NPG Asia Mater.* **2021**, *13*, 34.
- [30] J. Kim, G. Zhang, M. Shi, Z. Suo, *Science* **2021**, *374*, 212.
- [31] M. Rubinstein, R. H. Colby, *Polymer Physics*, Oxford University Press, Oxford, UK **2003**.
- [32] S. Wu, *J. Polym. Sci., Part B: Polym. Phys.* **1989**, *27*, 723.
- [33] M. M. Crowley, F. Zhang, J. J. Koleng, J. W. McGinity, *Biomaterials* **2002**, *23*, 4241.
- [34] C. Chen, Z. Wang, Z. Suo, *Extreme Mech. Lett.* **2017**, *10*, 50.
- [35] J. P. Gong, *Soft Matter* **2006**, *2*, 544.
- [36] J. P. Gong, G. Kagata, Y. Osada, *J. Phys. Chem. B* **1999**, *103*, 6007.
- [37] J. P. Gong, *Soft Matter* **2010**, *6*, 2583.
- [38] J.-Y. Sun, X. Zhao, W. R. K. Illeperuma, O. Chaudhuri, K. H. Oh, D. J. Mooney, J. J. Vlassak, Z. Suo, *Nature* **2012**, *489*, 133.
- [39] L. Xu, S. Gao, Q. Guo, C. Wang, Y. Qiao, D. Qiu, *Adv. Mater.* **2020**, *32*, 2004579.
- [40] X. Zhao, *Soft Matter* **2014**, *10*, 672.
- [41] P. Jiang, P. Lin, C. Yang, H. Qin, X. Wang, F. Zhou, *Chem. Mater.* **2020**, *32*, 9983.
- [42] J. P. Gong, Y. Katsuyama, T. Kurokawa, Y. Osada, *Adv. Mater.* **2003**, *15*, 1155.
- [43] Y. Tanaka, R. Kuwabara, Y.-H. Na, T. Kurokawa, J. P. Gong, Y. Osada, *J. Phys. Chem. B* **2005**, *109*, 11559.
- [44] R. E. Webber, C. Creton, H. R. Brown, J. P. Gong, *Macromolecules* **2007**, *40*, 2919.
- [45] S. Ahmed, T. Nakajima, T. Kurokawa, Md. A. Haque, J. P. Gong, *Polymer* **2014**, *55*, 914.
- [46] W. Zhang, X. Liu, J. Wang, J. Tang, J. Hu, T. Lu, Z. Suo, *Eng. Fract. Mech.* **2018**, *187*, 74.
- [47] S. Hong, D. Sycks, H. F. Chan, S. Lin, G. P. Lopez, F. Guilak, K. W. Leong, X. Zhao, *Adv. Mater.* **2015**, *27*, 4035.
- [48] E. A. Trowbridge, C. E. Crofts, *Biomaterials* **1987**, *8*, 201.
- [49] B. P. Pereira, P. W. Lucas, T. Swee-Hin, *J. Biomech.* **1997**, *30*, 91.
- [50] J. S. Grashow, A. P. Yoganathan, M. S. Sacks, *Ann. Biomed. Eng.* **2006**, *34*, 315.
- [51] F. Javid, N. Shahmansouri, J. Angeles, R. Mongrain, *Biomech. Model. Mechanobiol.* **2019**, *18*, 89.
- [52] G. J. Lake, A. G. Thomas, *Proc. R. Soc. London Ser. Math. Phys. Sci.* **1967**, *300*, 108.
- [53] J. Liu, C. Yang, T. Yin, Z. Wang, S. Qu, Z. Suo, *J. Mech. Phys. Solids* **2019**, *133*, 103737.
- [54] S. Lin, J. Ni, D. Zheng, X. Zhao, *Extreme Mech. Lett.* **2021**, *48*, 101399.
- [55] Z. Wang, C. Xiang, X. Yao, P. Le Floch, J. Mendez, Z. Suo, *Proc. Natl. Acad. Sci. USA* **2019**, *116*, 5967.
- [56] E. Di Giuseppe, in *Reference Module in Earth Systems and Environmental Sciences*, Elsevier, **2018**.
- [57] A. V. Reis, A. R. Fajardo, I. T. A. Schuquel, M. R. Guilherme, G. J. Vidotti, A. F. Rubira, E. C. Muniz, *J. Org. Chem.* **2009**, *74*, 3750.
- [58] Md. T. I. Mredha, H. H. Le, V. T. Tran, P. Trtik, J. Cui, I. Jeon, *Mater. Horiz.* **2019**, *6*, 1504.
- [59] M. Pike, W. F. Watson, *J. Polym. Sci.* **1952**, *9*, 229.